



Research articles

Spin-polarized-current switching mediated by Majorana bound states

V.V. Val'kov*, S.V. Aksenov

Kirensky Institute of Physics, Federal Research Center KSC SB RAS, 660036 Krasnoyarsk, Russia



ARTICLE INFO

Article history:

Received 4 December 2017

Received in revised form 26 March 2018

Accepted 18 April 2018

Available online 1 June 2018

Keywords:

Majorana bound states

Topological superconductivity

Current-switch effect

ABSTRACT

We present the study of transport properties of a superconducting wire with strong Rashba spin-orbit coupling for different orientations of an external magnetic field. Using the nonequilibrium Green's functions in the tight-binding approach the crucial impact of the relative alignment of lead magnetization and the Majorana bound state (MBS) spin polarization on the low-bias conductance and shot noise is presented. Depending on this factor the transport regime can effectively vary from symmetric to extremely asymmetric. In the last situation the suppression of MBS-assisted conductance results in current-switch effect allowing the electrical detection of the Majorana fermions.

© 2018 Published by Elsevier B.V.

1. Introduction

The pursuit of experimental observation of a Majorana fermion, originally started in the particle physics, continued then in the solid-state systems [1]. It was shown in the Kitaev model [2] that the emergent quasiparticles appearing in superconducting (SC) system possess the self-Hermitian property of the Majorana fermions. Majorana bound states (MBSs) in low-dimensional structures are spatially separated. The last feature opens a way to utilize the MBSs as the building blocks of fault-tolerant quantum computers [3]. Since the MBSs obey non-Abelian statistics [4] an MBS-based qubit can be manipulated by braiding operations [5].

Among different systems where MBSs were predicted semiconducting wires with strong spin-orbit coupling (SOC) and in proximity to an s-wave SC [6,7] attract considerable attention since the corresponding experimental proofs were provided [8]. Under the influence of an external magnetic field an effective p-wave pairing is realized in the wire and two MBSs appear at its opposite ends [6,7]. In addition to studying the fundamental properties of MBS in the wires, a number of applications was already proposed, e.g. memory cell [9], current switch [10], rectifier and Cooper pair splitter [11,12].

The tunneling spectroscopy measurements reveal the zero-bias conductance peak (ZBP) indicating resonant Andreev transport processes through the zero-energy MBS [13,8]. Furthermore, the shot noise provides supplementary information about the MBSs [14,15]. It is essential that the Majorana nature of the ZBP is not

a single interpretation [16]. Therefore, it is necessary to analyze supplementary information concerning quantum transport via the MBSs. One of such properties is an electronic spin polarization in the MBS [17] which we call here the MBS spin polarization. In the present article the influence of MBS spin polarization on non-local quantum transport is analyzed. Studying spin-polarized transport we show that the low-bias conductance brings the features allowing both to detect the MBSs and employ that unusual behavior in electronic applications such as a current switch. In Ref. [10] the current switch assisted by the MBSs was already studied. The effect was induced by the combination of quantum phase transition and destructive interference. In contrast, our proposal is based on the features of MBS spin polarization as it is shown in Fig. 1. While the local character of the magnetic field in the proposed scheme can present a certain obstacle for its experimental realization we suggest to apply a magnetic gate to overcome this problem. Note that the scheme containing ferromagnets for the MBS electrical detection was also proposed in Ref. [18]. However, their role differs in principle from the one considered here. In our situation the presence of ferromagnets is not vital to induce the MBSs but is necessary to probe nonlocal transport.

2. The model Hamiltonian

Let us consider a nanowire with the strong Rashba SOC deposited on a grounded s-type SC (see Fig. 1). Hereinafter we name it a 'superconducting wire' taking into account an induced SC pairing in the wire characterized by a parameter Δ . An external magnetic field $\mathbf{B} = (B_x, 0, -B_z) = B(\cos \theta, 0, -\sin \theta)$ is assumed to be oriented at an arbitrary angle in the plane perpendicular to the Rashba field $\mathbf{B}_{\text{SO}} \parallel \mathbf{y}$. We suppose in electronic applications the direction and

* Corresponding author

E-mail addresses: vvv@iph.krasn.ru (V.V. Val'kov), asv86@iph.krasn.ru (S.V. Aksenov).

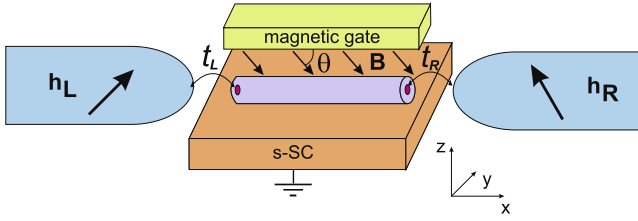


Fig. 1. The superconducting wire between ferromagnetic leads. Red circles indicate the MBSs.

amplitude of magnetic field can be manipulated by a 'magnetic gate', e.g. as it was proposed to manipulate domain-wall motion in [19].

The microscopic Hamiltonian of SC wire is

$$\hat{H}_W = \sum_{j=1}^N \left[\sum_{\sigma} \xi_{\sigma} a_{j\sigma}^{\dagger} a_{j\sigma} + \Delta a_{j1} a_{j2} - V_x a_{j1}^{\dagger} a_{j2} + H.c. \right] - \sum_{\sigma, j=1}^{N-1} \left[\frac{t}{2} a_{j\sigma}^{\dagger} a_{j+1, \sigma} + \frac{\alpha}{2} \sigma a_{j\sigma}^{\dagger} a_{j+1, \bar{\sigma}} + H.c. \right], \quad (1)$$

where $a_{j\sigma}$ – an electron annihilation operator on j th site of the wire with spin σ ; $\xi_{\sigma} = t + \sigma V_z - \mu$ – an on-site energy of the electron with spin σ taking into account the Zeeman component V_z ; μ – a chemical potential of the system; $V_{x(z)} = \mu_B B_{x(z)}$ – x - and z -components of the Zeeman energy; t – a nearest neighbor hopping parameter; α – an intensity of the Rashba SOC.

The SC wire is situated between the ferromagnetic leads characterized by the Stoner-type Hamiltonians:

$$\hat{H}_i = \sum_{k\sigma} \{ [\xi_k - eV_i - \sigma M_i \cos \theta_i] c_{k\sigma}^{\dagger} c_{k\sigma} - M_i \sin \theta_i c_{k\sigma}^{\dagger} c_{k\bar{\sigma}} \}, i = L, R, \quad (2)$$

where $c_{k\sigma}^{\dagger}$ – an electron creation operator in i th lead with a wave vector k , spin σ and an energy $\xi_k = \epsilon_k - \mu$; $M_i = \frac{1}{2} g \mu_B h_i$ – an energy of the i th lead magnetization \mathbf{h}_i ; θ_i – an angle between \mathbf{h}_i and z axis in the xz plane; $\sigma = \pm 1$ or \uparrow, \downarrow . The bias voltage $V_{L(R)} = \pm V/2$ is applied to the left (right) lead.

The interaction between the leads and the SC wire is given by a standard tunnel Hamiltonian,

$$\hat{H}_T = t_L \sum_{k\sigma} c_{k\sigma}^{\dagger} a_{1\sigma} + t_R \sum_{p\sigma} c_{p\sigma}^{\dagger} a_{N\sigma} + H.c., \quad (3)$$

where $t_{L(R)}$ – a tunnel parameter between the left (right) lead and the wire. Thus, the total Hamiltonian of the system is $\hat{H} = \hat{H}_L + \hat{H}_R + \hat{H}_T + \hat{H}_W$.

3. Current and noise in terms of the nonequilibrium Green's functions

To calculate spin-dependent transport properties of the SC wire we employ the nonequilibrium Green's functions [20,21] in the spin \otimes Nambu space [22]. After some manipulations the general expression describing current in the i th lead can be written as following

$$\langle \hat{I}_i \rangle = e \int_{-\infty}^{+\infty} \frac{d\omega}{\pi} \text{Tr} \left[\text{Re} \left\{ \hat{\sigma} \left(\hat{\Sigma}_i^r \hat{G}_{ii}^< + \hat{\Sigma}_i^< \hat{G}_{ii}^a \right) \right\} \right], \quad (4)$$

where $\hat{\sigma} = \text{diag}(1, -1, 1, -1)$ accounts for the electron and hole transport channels; $\hat{\Sigma}_i^{r,<} = \hat{T}_i^{\dagger} \hat{g}_i^{r,<} \hat{T}_i$ – the Fourier transform of matrix retarded/lesser self-energy function describing the influence of i th lead on the wire; $\hat{g}_i^{r,<} = \hat{T}_i^{\dagger} \hat{g}_i^{r,<} \hat{T}_i$ – the Fourier transform of matrix retarded/lesser of free-particle Green's function of i th lead. In this

work we consider half-metallic leads (e.g. NiMnSb or CrO₂ [23]) where $\theta_i = 0$. Consequently, the time-dependent tunnel coupling matrices are $\hat{T}_i(t) = \frac{1}{2} \text{diag}(e^{-ieV_i t}, -e^{ieV_i t}, e^{-ieV_i t}, -e^{ieV_i t})$. $\hat{G}_{ii}^{<,a} = \hat{P}_i \hat{G}_W^{<,a} \hat{P}_i^{\dagger}$ – the Fourier transforms of the lesser/advanced Green's functions of the wire which are projected on the subspace of site tunnel-coupled with the i th lead. To obtain $\hat{G}_{ii}^{<,a}$ the projection operators $\hat{P}_L = (\hat{I}\hat{O})$, $\hat{P}_R = (\hat{O}\hat{I})$ are used, where $\hat{I} - 4 \times 4$ unit matrix; $\hat{O} - 4 \times 4N - 4$ zero block [24].

The nonequilibrium Green's functions can be obtained from the Dyson and Keldysh equations,

$$\hat{G}_W^r = (\omega - \hat{h}_W - \hat{\Sigma}^r)^{-1}, \hat{G}_W^a = (\hat{G}_W^r)^{\dagger}, \quad (5)$$

$$\hat{G}_W^< = \hat{G}_W^r \hat{\Sigma}^< \hat{G}_W^a. \quad (6)$$

In expressions (5), (6) \hat{h}_W is the matrix of Hamiltonian (1) in the spin \otimes Nambu space. The total self-energy function of the system is $\hat{\Sigma}^n = \hat{P}_L^{\dagger} \hat{\Sigma}_L^n \hat{P}_L + \hat{P}_R^{\dagger} \hat{\Sigma}_R^n \hat{P}_R$. The i th lead components are $\Sigma_i^r = -\frac{i}{2} \Gamma_i$, $\hat{\Sigma}_i^< = (\Sigma_i^a - \Sigma_i^r) \hat{F}_i$, where $\Gamma_i = 2\pi (\frac{t_i}{2})^2 \rho_i$ – the coupling strength between the wire and the majority subband of i th lead; ρ_i – the DOS of majority subband of i th lead. In the calculations below the leads are treated in the wide-band limit that results in $\Gamma_i = \text{const}$. Finally, $\hat{F}_i = \text{diag}(n_{i1}, n_{i2}, n_{i1}, n_{i2})$, where $n_{i1,2}(\omega \pm eV_i)$ – the Fermi distribution functions.

Additionally, we analyze the autocorrelations of the current in the leads. In particular, the noise spectral density in the left lead can be written as

$$S_i(\omega) = \int dt e^{i\omega t} \langle \delta I_i(t) \delta I_i(0) + \delta I_i(0) \delta I_i(t) \rangle. \quad (7)$$

Substituting (4) into (7) the zero-frequency shot noise is given by [22,25]

$$S_i(\omega) = 2e^2 \int_{-\infty}^{+\infty} \frac{d\omega}{2\pi} \text{Tr} \left[\hat{\sigma} \hat{\Sigma}_i^< \hat{\sigma} \hat{G}_{ii}^> + \hat{G}_{ii}^< \hat{\sigma} \hat{\Sigma}_i^> \hat{\sigma} - \hat{\sigma} \left[\hat{\Sigma}_i \hat{G}_{ii} \right]^< \hat{\sigma} \left[\hat{\Sigma}_i \hat{G}_{ii} \right]^> - \left[\hat{G}_{ii} \hat{\Sigma}_i \right]^< \hat{\sigma} \left[\hat{G}_{ii} \hat{\Sigma}_i \right]^> \hat{\sigma} + \hat{\sigma} \left[\hat{\Sigma}_i \hat{G}_{ii} \hat{\Sigma}_i \right]^> \hat{\sigma} \hat{G}_{ii}^< + \hat{G}_{ii}^> \hat{\sigma} \left[\hat{\Sigma}_i \hat{G}_{ii} \hat{\Sigma}_i \right]^< \hat{\sigma} \right]. \quad (8)$$

In many works concerning the topologically SC wires the relation between the parameters of system is typically $t \gg \alpha, V_{x,z}, \Delta$ [8,22]. We choose slightly different condition $t \sim \alpha, V_{x,z}, \Delta$ which results in the increase of oscillation period of MBS zero mode energy and considerably simplifies the transport calculations. The transport is analyzed at low temperatures $kT = 10^{-10}$ and low bias $eV \sim E_M$ where E_M is the MBS energy. Therefore and for the sake of simplicity, out of the parametric area where the topologically non-trivial is realized, $\mu^2 + \Delta^2 < V_x^2 + V_z^2 < (2t - \mu)^2 + \Delta^2$ [6,7,26], all physical quantities are set equal to zero. The hopping parameter $t = 1$ is in energy units.

4. Current-switch effect

To understand the features of transport properties we, firstly, analyze the MBS spin-up probability densities at both edges of the SC wire employing the Bogolubov transformation,

$$\beta_l = \sum_{n=1}^N \left[u_{ln} a_{n1} + v_{ln} a_{n1}^{\dagger} + w_{ln} a_{n1} + z_{ln} a_{n1}^{\dagger} \right]. \quad (9)$$

In Fig. 2a, b the MBS spin-up probability densities at the left and right end sites of the wire, $P_{M,L(R)1}$, are demonstrated as functions of the magnetic-field orientation and amplitude. According to the

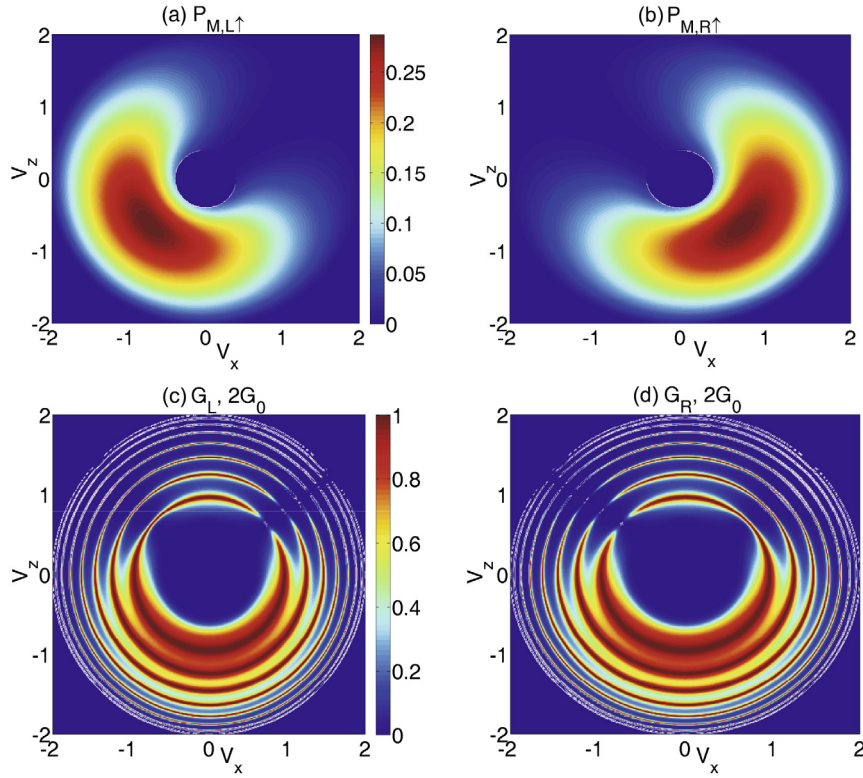


Fig. 2. The magnetic-field orientation dependence of the MBS spin-up probability densities (a and b) and low-bias conductance (c and d). Parameters: $\mu = 0, \Delta = 0.4, \alpha = 2, N = 30$.

wire's Hamiltonian (1), $P_{M,L(R)\uparrow} = 2|u_{M,1(N)}|^2 (|u_{M,1(N)}| \simeq |z_{M,1(N)}|)$ have maxima at the lower part of maps and are suppressed in the opposite fields. Simultaneously, the maxima of $P_{M,i\uparrow}$ at opposite edges for given V_z appear at the opposite longitudinal fields. It is worth to note that the calculation of MBS spin polarization $P_{M,i} = P_{M,i\uparrow} - P_{M,i\downarrow}$ gives the numerical results which just quantitatively differ from the ones based on the rigorous definition [17,26,27].

Now we turn to the behavior of MBS-assisted conductance and noise. In spin-polarized regime the transport is strongly determined by the effective coupling strengths which include the information about the spin-dependent lifetime of the MBSs proportional to $P_{M,L(R)\uparrow}$. This is confirmed by the magnetic-field orientation dependencies of the low-bias ($eV = 10^{-4}$) conductances of left and right leads in Fig. 2c and d, respectively. Both maps look similar as the sequences of concentric rings where the conductance is about $2G_0$ (hereinafter the MBS rings). Such peculiarities are the result of resonant transport via the MBSs [13,22]. The periodical appearance of the conductance maximum with changing magnetic-field amplitude is in agreement with the oscillations of E_M caused by the magnetic-field periodical dependence of the coupling between the MBSs, t_y [28].

Since there are only spin-up carriers in the leads the effective couplings with the wire and the conductances are greater in the lower half-plane, according to the model Hamiltonian (1). In general, the conductance of the contact with topologically SC system is greater if the lead's polarization is parallel to the magnetic field [29]. In the upper half-plane the MBS rings of G_L and G_R become thinner and the breaks appear for two magnetic-field orientations, $V_x \approx \pm V_z$, respectively. Thus, we get obvious current-symmetry breaking, $I_L \neq -I_R$. Such a situation in charge nonconserving system is not realized in the symmetric coupling and voltage regime, $\Gamma_L = \Gamma_R$ and $V_L = V_R$, if leads are paramagnetic [30].

In our system perfectly spin-polarized current from the left (right) lead is significantly hampered due to the vanishing same-spin MBS probability density at the left (right) wire's end. As a result, the left (right) effective coupling strength is extremely decreased and the regime turns to be strongly asymmetric at $V_x \approx \pm V_z$. Consequently, at both orientations the transport properties of the system are qualitatively similar to those observed at one-lead geometry. For example, if $V_x \approx V_z$ the wire is virtually connected only with the right lead. Then G_L is close to zero and G_R tends to unity in the MBS rings.

The current-noise calculations display asymmetry as well. The left Fano factor, $F_L = S_L/2eI_L$, approaches 2 at low conductance if $V_x \approx -V_z$ (see the red noise trail at Fig. 3). One points out that the transport in this case is predominantly mediated by local Andreev reflection and is typical for one-lead regime. The Fano factors corresponding to the MBS rings are zero indicating the Majorana-induced resonant Andreev tunneling [22].

From experimental point of view the conductance of the SC wire, $G = \frac{1}{2} \frac{d}{dV} (I_L - I_R) = \frac{1}{2} (G_L + G_R)$, is more interesting. Taking into account the behavior of G_L and G_R (Fig. 2c, d) we see that the height of the MBS rings of G for the two magnetic-field orientations, $V_z \approx \pm V_x$, is G_0 instead of $2G_0$ when $V_z \neq V_x$. In other words, the direction of the current in the SC substrate, $-I_0 = I_L + I_R$, can be controlled by the magnetic field. If $V_z \approx V_x$ and $eV/2 > E_M$ that $I_L \approx 0$ (since in the low-bias regime only the MBS participates at transport), $I_0 \approx |I_R|$ as it is shown in Fig. 4a. Similarly, if $V_z \approx -V_x$ and $eV/2 > E_M$ that $I_R \approx 0, I_0 \approx -|I_L|$ (Fig. 4b). Finally, if $V_x \neq \pm V_z$ and $eV/2 > E_M$ that $I_L \approx -I_R$ and $I_0 \approx 0$ (Fig. 4c). In contrast to [31] the conductance corresponding to I_0 is not zero for $V_z \approx \pm V_x$ if the coupling of the SC wire with the leads is symmetric, $\Gamma_L = \Gamma_R$, and is approximately equal to $2G_0$. Thus, the effect of the current switch can be used to detect Majorana fermions and in electronic applications.

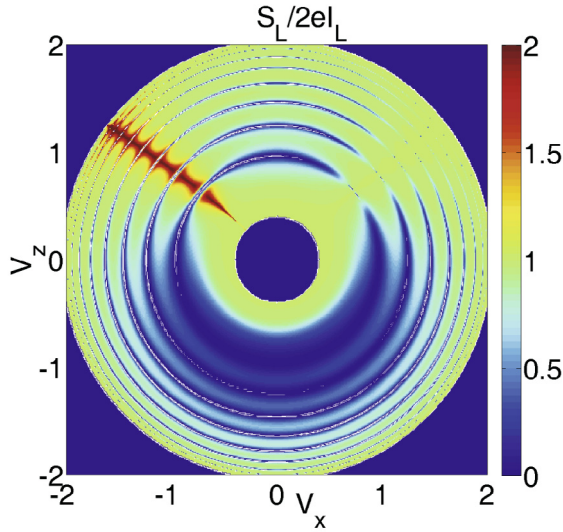


Fig. 3. The magnetic-field orientation dependence of the left-lead Fano factor. Parameters are the same as in Fig. 2.

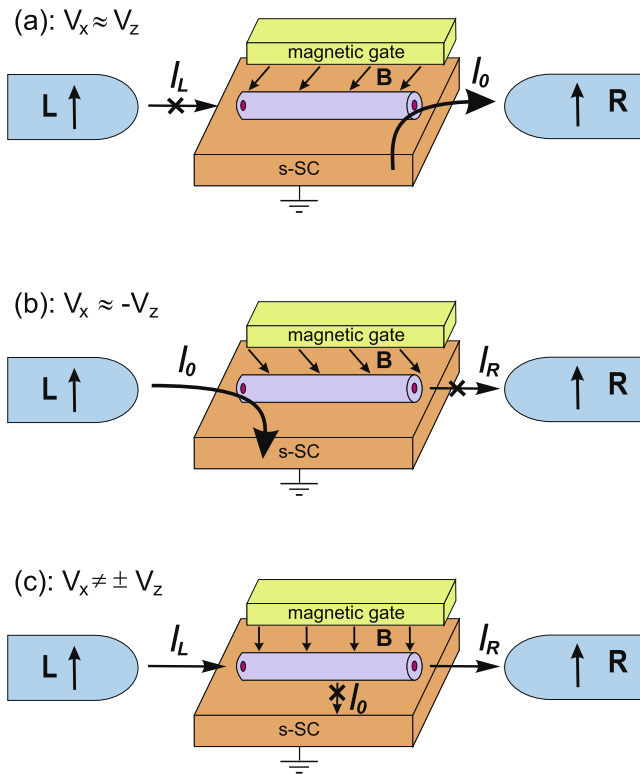


Fig. 4. The scheme of the MBS-assistant current switch. (a) $I_L \rightarrow 0$ and $I_0 \approx -I_R$ since $P_{ML} = P_{M,L}$ and $\theta_L = 0$ for $V_x > 0, V_z \approx V_x$; (b) $I_R \rightarrow 0$ and $I_0 \approx -I_L$ since $P_{MR} = P_{M,R}$ and $\theta_R = 0$ for $V_x < 0, V_z \approx -V_x$; (c) $I_0 \rightarrow 0$ and $I_L \approx -I_R$ if $V_x \neq \pm V_z$.

5. Conclusion

We studied the influence of the magnetic-field orientation on spin-polarized quantum transport in the SC wire. Using the nonequilibrium Green's functions and microscopic tight-binding description of the SC wire it is demonstrated that the width of MBS rings in the lead conductance increases for the magnetic-field orientations in which the lead magnetization and the MBS spin polarization at the adjacent wire edge are oriented in the same

direction. If they are antiparallel the corresponding conductance vanishes. Simultaneously, the MBS rings in the conductance of opposite lead survive and the corresponding Fano factor displays specific noise trail indicating the domination of the MBS-assisted local Andreev reflection processes. These effects give rise to strong current asymmetry in the system. Taking it into account we propose the MBS-assisted current switch device where charge carrier flow can be controlled by magnetic gate. There are three possible paths of the current: (a) from the substrate to the right lead if $V_x \approx V_z$; (b) from the left lead to the substrate if $V_x \approx -V_z$; (c) from the left to right lead if $V_x \neq \pm V_z$.

Acknowledgment

We acknowledge fruitful discussions with A.D. Fedoseev and M. S. Shustin. The work was supported by the Comprehensive Programme SB RAS No. 0356-2015-0403, Russian Foundation for Basic Research, Government of Krasnoyarsk Territory, Krasnoyarsk Region Science and Technology Support Fund to the research projects Nos. 16-02-00073, 17-42-240441. The work of S.V.A. was supported by grant of the President of the Russian Federation (MK-1398.2017.2).

References

- [1] S.R. Elliott, M. Franz, Rev. Mod. Phys. 87 (2015) 137, <https://doi.org/10.1103/RevModPhys.87.137>.
- [2] A.Y. Kitaev, Phys. Usp. 44 (2001) 131, <https://doi.org/10.1070/1063-7869/44/105/S29>.
- [3] A.Y. Kitaev, Ann. Phys. 303 (2003) 2, [https://doi.org/10.1016/S0003-4916\(02\)00018-0](https://doi.org/10.1016/S0003-4916(02)00018-0).
- [4] D.A. Ivanov, Phys. Rev. Lett. 86 (2001) 268, <https://doi.org/10.1103/PhysRevLett.86.268>.
- [5] J. Alicea, Y. Oreg, G. Refael, F. von Oppen, M.P.A. Fisher, Nat. Phys. 7 (2011) 412, <https://doi.org/10.1038/NPHYS1915>.
- [6] R.M. Lutchyn, J.D. Sau, S.D. Sarma, Phys. Rev. Lett. 105 (2010) 077001, <https://doi.org/10.1103/PhysRevLett.105.077001>.
- [7] Y. Oreg, G. Refael, F. von Oppen, Phys. Rev. Lett. 105 (2010) 177002, <https://doi.org/10.1103/PhysRevLett.105.177002>.
- [8] V. Mourik, K. Zuo, S.M. Frolov, S.R. Plissard, E.P.A.M. Bakkers, L.P. Kouwenhoven, Science 336 (2012) 1003, <https://doi.org/10.1126/science.1222360>.
- [9] T. Hyart, B. van Heck, I.C. Fulga, M. Burrello, A.R. Akhmerov, C.W.J. Beenakker, Phys. Rev. B 88 (2013) 035121, <https://doi.org/10.1103/PhysRevB.88.035121>.
- [10] F.A. Dessotti, L.S. Ricco, Y. Marques, L.H. Guessi, M. Yoshida, M.S. Figueira, M. de Souza, P. Sodano, A.C. Seridonio, Phys. Rev. B 94 (2016) 125426, <https://doi.org/10.1103/PhysRevB.94.125426>.
- [11] J.J. He, J. Wu, T.-P. Choy, X.-J. Liu, Y. Tanaka, K.T. Law, Nat. Commun. 5 (2014) 3232, <https://doi.org/10.1038/ncomms4232>.
- [12] T.O. Rosdahl, A. Vuik, M. Kjaergaard, A.R. Akhmerov, e-print arXiv:1706.08888, 2017 [cond-mat.mes-hall].
- [13] K. Flensberg, Phys. Rev. B 82 (2010), <https://doi.org/10.1103/PhysRevB.82.180516>, 180516(R).
- [14] J. Nilsson, A.R. Akhmerov, C.W.J. Beenakker, Phys. Rev. Lett. 101 (2008) 120403, <https://doi.org/10.1103/PhysRevLett.101.120403>.
- [15] C.W.J. Beenakker, Rev. Mod. Phys. 87 (2015) 1037, <https://doi.org/10.1103/RevModPhys.87.1037>.
- [16] D. Bagrets, A. Altland, Phys. Rev. Lett. 109 (2012) 227005, <https://doi.org/10.1103/PhysRevLett.109.227005>.
- [17] D. Sticlet, C. Bena, P. Simon, Phys. Rev. Lett. 108 (2012) 096802, <https://doi.org/10.1103/PhysRevLett.108.096802>.
- [18] A.R. Akhmerov, J. Nilsson, C.W.J. Beenakker, Phys. Rev. Lett. 102 (2009) 216404, <https://doi.org/10.1103/PhysRevLett.102.216404>.
- [19] C. Murapaka, P. Sethi, S. Goolaup, W.S. Lew, Sci. Rep. 6 (2016) 20130, <https://doi.org/10.1038/srep20130>.
- [20] L.V. Keldysh, J. Theor. Exp. Phys. 20 (1965) 1018.
- [21] S. Datta, Quantum Transport: Atom to Transistor, Cambridge University Press, New York, 2005.
- [22] B.H. Wu, J.C. Cao, Phys. Rev. B 85 (2012) 085415, <https://doi.org/10.1103/PhysRevB.85.085415>.
- [23] R.S. Keizer, S.T.B. Goennenwein, T.M. Klapwijk, G. Miao, G. Xiao, A. Gupta, Nature 439 (2006) 825, <https://doi.org/10.1038/nature04499>.
- [24] M.Y. Kagan, V.V. Val'kov, S.V. Aksenov, Phys. Rev. B 95 (2017) 035411, <https://doi.org/10.1103/PhysRevB.95.035411>.
- [25] V.A. Khlus, Sov. Phys. JETP 66 (1987) 1243.
- [26] V.V. Val'kov, S.V. Aksenov, Low Temp. Phys. 43 (2017) 436, <https://doi.org/10.1063/1.4983331>.

- [27] V.V. Val'kov, S.V. Aksenov, *J. Magn. Magn. Mater.* 440 (2017) 112, <https://doi.org/10.1016/j.jmmm.2016.10.155>.
- [28] S.D. Sarma, J.D. Sau, T.D. Stanescu, *Phys. Rev. B* 86 (2012) 220506(R), <https://doi.org/10.1103/PhysRevB.86.220506>.
- [29] H.-H. Sun, K.-W. Zhang, L.-H. Hu, C. Li, G.-Y. Wang, H.-Y. Ma, Z.-A. Xu, C.-L. Gao, D.-D. Guan, Y.-Y. Li, C. Liu, D. Qian, Y. Zhou, L. Fu, S.-C. Li, F.-C. Zhang, J.-F. Jia, *Phys. Rev. Lett.* 116 (2016) 257003, <https://doi.org/10.1103/PhysRevLett.116.257003>.
- [30] J.-B. You, X.-Q. Shao, Q.-J. Tong, A.H. Chan, C.H. Oh, V. Vedral, *J. Phys.: Condens. Matter* 27 (2015) 225302, <https://doi.org/10.1088/0953-8984/27/22/225302>.
- [31] Y. Cao, P. Wang, G. Xiong, M. Gong, X.-Q. Li, *Phys. Rev. B* 86 (2012) 115311, <https://doi.org/10.1103/PhysRevB.86.115311>.